

High-resolution photoelectron spectroscopy and calculations of the highest bound levels of D-2(+) below the first dissociation threshold

Journal Article**Author(s):**

Beyer, Maximilian; Merkt, Frédéric

Publication date:

2017-08-14

Permanent link:

<https://doi.org/10.3929/ethz-b-000190271>

Rights / license:

In Copyright - Non-Commercial Use Permitted

Originally published in:

Journal of Physics B: Atomic, Molecular and Optical Physics 50(15), <https://doi.org/10.1088/1361-6455/aa7ac9>

Funding acknowledgement:

743121 - Cold Ion Chemistry - Experiments within a Rydberg Orbit (EC)

172620 - Precision measurements with cold molecules: Rydberg states, ions and photoionization (SNF)

This article may be downloaded for personal use only. Any other use requires prior permission of the author and IOP Publishing.

The following article appeared in *J. Phys. B: At. Mol. Opt. Phys.* **50**, 154005 (2017) and may be found at <http://iopscience.iop.org/article/10.1088/1361-6455/aa7ac9>

High-resolution photoelectron spectroscopy and calculations of the highest bound levels of D_2^+ below the first dissociation threshold

Maximilian Beyer and Frédéric Merkt

Laboratorium für Physikalische Chemie, ETH Zürich, 8093 Zürich, Switzerland

(Dated: May 23, 2017)

Pulsed-field ionization zero-kinetic-energy photoelectron spectra of D_2 have been recorded from the intermediate $\bar{H} \ ^1\Sigma_g^+$ state to determine the positions of bound rovibronic levels of D_2^+ located up to 1400 cm^{-1} below the $D^+ + D(1s)$ dissociation threshold. The ion-pair character of the \bar{H} intermediate state resulted in large changes $\Delta N = N^+ - N$ of the rotational quantum number upon photoionization, which enabled the observation of levels of D_2^+ with rotational quantum number N^+ as high as 10. The experimental data cover a range of levels within which the usual hierarchy of timescales of the electronic, vibrational and rotational motions is inverted. The term values of these levels with respect to the $X \ ^1\Sigma_g^+(v = 0, N = 0)$ rovibronic ground state of D_2 and the energy intervals of the ionic states, measured with an accuracy of typically 0.11 cm^{-1} and 0.02 cm^{-1} , respectively, are compared with positions calculated ab-initio at various degrees of approximation, starting from the Born-Oppenheimer approximation and successively including adiabatic, nonadiabatic, relativistic and radiative corrections. The comparison shows that the accuracy of the photoelectron-spectroscopic measurement is sufficient to reveal the effects of the adiabatic, nonadiabatic, relativistic and radiative corrections on the absolute term values. Comparing our calculations, which rely on an approximate evaluation of the nonadiabatic corrections based on effective R -dependent reduced masses, with the theoretical results for $N^+ \leq 5$ by Moss (*J. Chem. Soc. Faraday Trans.* **89**, 3851 (1993)) and for $N^+ \leq 8$ by Wolniewicz and Orlikowski (*Mol. Phys.* **74**, 103 (1991)) enables the quantification of the errors introduced by our approximative treatment of the nonadiabatic corrections. Improved rotational term values of the $\bar{H}(v = 12)$ level were also derived.

I. INTRODUCTION

H_2 , HD, D_2 and their positively charged ions H_2^+ , HD^+ and D_2^+ represent molecular systems of fundamental interest to test the accuracy limits of *ab initio* quantum-chemical calculations. Accurate *ab initio* predictions have been reported for a broad range of electronic, vibrational and rotational levels of these molecules, see e.g. Refs. 1–12. The most precise predictions are generally obtained for the lowest degree of excitation.

In the case of the cations, the experimental data available for comparison with the theoretical results are limited. So far, high-resolution spectroscopic data on D_2^+ are restricted to rovibronic transitions between the few bound levels of the $\text{A}^+ \ ^2\Sigma_u^+$ state and the highest rovibrational levels of the $\text{X}^+ \ ^2\Sigma_g^+$ state [13–15], and to the hyperfine structure of the ground state of para D_2^+ [16]. This paucity of data is the result of the zero permanent dipole moment of D_2^+ and the resulting absence of vibrational and pure rotational electric-dipole transitions.

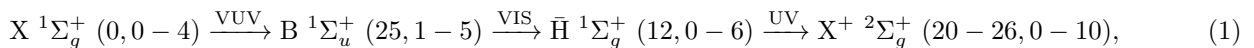
The purpose of the present article is to report a new measurement of a wide range of rovibrational levels of the X^+ and A^+ states of D_2^+ by pulsed-field ionization zero-kinetic-energy (PFI-ZEKE) photoelectron spectroscopy. The new data, which complement similar data obtained for H_2^+ in a recent study [17, 18], consist of 65 and 5 rovibrational levels of the $\text{X}^+ \ ^2\Sigma_g^+$ and $\text{A}^+ \ ^2\Sigma_u^+$ state of D_2^+ with v^+ between 20–26 and $N^+ = 0 - 10$, and $v^+ = 0, 1$ and $N^+ = 0 - 3$, respectively. The term values with respect to the $\text{X} \ ^1\Sigma_g^+$ ($v = 0, N = 0$) ground state of D_2 and the intervals between the rovibronic levels of D_2^+ were determined with typical uncertainties of 0.11 cm^{-1} and 0.02 cm^{-1} , respectively. These uncertainties are sufficiently small to reveal the effects of adiabatic, nonadiabatic, relativistic and radiative corrections. In particular, we investigate the effects of approximate treatments of the nonadiabatic corrections based on effective reduced masses. Such treatments are known to be less accurate than variational calculations, but they offer advantages when computing one-channel resonance phenomena and the associated dynamics, because they preserve a single-potential description of the electronic states [17, 18].

This investigation is part of an endeavor to determine the energy-level structure of simple molecular ions with the highest possible accuracy, both experimentally and theoretically. By exciting molecular Rydberg states of the neutral species belonging to series converging to the different rovibrational states of the ion, we overcome the problem of a vanishing permanent dipole moment that complicates the direct spectroscopic study on the ion. In addition, the use of multiphoton-excitation sequences allows us to probe molecular geometries that one could not reach directly from the rovibronic ground state because of vanishing Franck-Condon factors.

The focus of the present article lies on energy levels of D_2^+ located close to the dissociation limit. In combination with Rydberg states of high principal quantum number this opens up the prospect of studying molecular systems in a range of energies and particle distances where both the electronic and nuclear motions approach their respective continuum.

II. EXPERIMENTAL METHODS

The experiment relied on the use of PFI-ZEKE photoelectron spectroscopy in combination with a resonant three-photon-excitation scheme from the ground $\text{X} \ ^1\Sigma_g^+$ ($v = 0$) state of D_2 via excited vibrational levels of the $\text{B} \ ^1\Sigma_u^+$ and $\bar{\text{H}} \ ^1\Sigma_g^+$ states,



as described in our previous reports on H_2^+ [17, 18] and depicted schematically in Fig. 1. This sequence utilizes the $\bar{\text{H}}$ outer well of the $\text{H}\bar{\text{H}} \ ^1\Sigma_g^+$ state of H_2 to reach the highest vibrational states of H_2^+ by threshold ionization. The numbers in parentheses in Eq. (1), given after the state labels, indicate the vibrational and rotational quantum numbers in the notation (v, N) .

This excitation scheme enables one to reach highly excited vibrational levels of the $\text{X}^+ \ ^2\Sigma_g^+$ state by gradually increasing the internuclear distance. Rovibronic photoionization selection rules permit the observation of transitions with $\Delta N = N^+ - N$ up to six because of the ion-pair character of the $\bar{\text{H}}$ intermediate state (see Section IV).

The VUV, visible and UV laser radiation used to drive the transitions was generated using commercial Nd:YAG-pumped pulsed dye lasers (repetition rate 25 Hz) in combination with suitable nonlinear frequency-up-conversion schemes, as described in Ref. 17. The UV-laser pulses were delayed by 10 ns with respect to the other laser pulses in order to decrease the probability of direct single-photon ionization from the B state, which has a lifetime of less than 1 ns [19]. The PFI-ZEKE photoelectron spectra were recorded using a delayed multipulse field-ionization sequence, as described in Ref. 20. The full width at half maximum of the narrowest lines of the photoelectron spectrum was 0.1 cm^{-1} . The pulse sequence, consisting of a discrimination pulse followed by nine field-ionization pulses of increasing field strength, enabled the recording of several PFI-ZEKE photoelectron spectra per laser scan, each characterized by

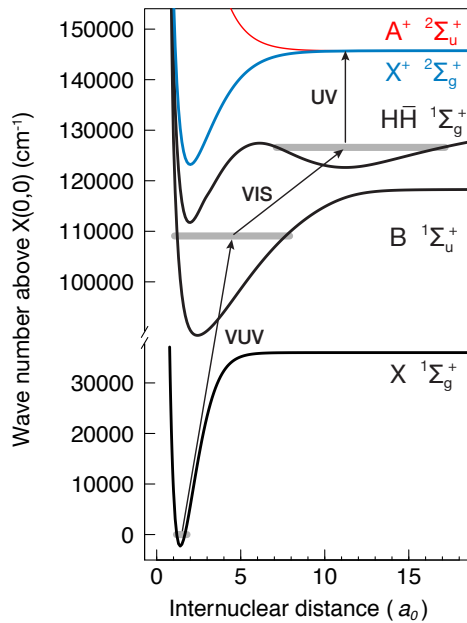


FIG. 1. Excitation sequence showing the resonant three-photon excitation of molecular Rydberg states in the vicinity of the first dissociation threshold of D_2^+ from the $X \ ^1\Sigma_g^+$ ground state of D_2 via the intermediate $B \ ^1\Sigma_u^+$ and $H\bar{H} \ ^1\Sigma_g^+$ states.

a specific shift of the ionization thresholds. The spectra obtained with the two largest field-ionization pulses were not used in the statistical analysis despite their excellent signal-to-noise ratio because of the slightly asymmetric lineshape caused by the n dependence of the lifetimes of the Rydberg states probed by these pulses.

The UV wave number was calibrated using a wavemeter (absolute accuracy of 0.02 cm^{-1} , relative accuracy of 0.015 cm^{-1}) and the line centers were determined using a Poisson-weighted nonlinear fit of a Gaussian line-shape model assuming a constant line width for a given field-ionization pulse. The relative positions of the rovibronic levels of D_2^+ were extracted in a weighted linear least-squares fit from a redundant network of transitions connecting different rotational levels of the $\bar{H}(v=12)$ state to the rovibronic ionization thresholds. The absolute term values of the D_2^+ levels with respect to the $X \ ^1\Sigma_g^+(0,0)$ ground state of D_2 were obtained by adding the calibrated UV wave numbers to the term values of the $\bar{H}(12, N)$ levels reported by Reinhold *et al.* [21] and compensating for the shift of the ionization thresholds induced by the pulsed field ionization [20]. This procedure resulted in typical absolute and relative uncertainties of 0.11 cm^{-1} and 0.02 cm^{-1} , respectively, for the rovibronic levels of D_2^+ .

III. CALCULATION OF DISSOCIATION ENERGIES OF THE BOUND LEVELS OF D_2^+

For the calculations of the dissociation energies, we follow the procedure described in Ref. 18 and therefore only give a very brief outline here. Atomic units are used. For the deuteron-to-electron mass ratio m_d , E_h , and α , we used $m_d = 3670.48296785(13)$, $E_h/hc = 219474.6313702(13) \text{ cm}^{-1}$ and $\alpha^{-1} = 137.035999139(31)$, respectively [23]. Bound-state energies were obtained by integrating the nuclear Schrödinger equation

$$\left[-\frac{1}{2\mu_{\text{vib}}} \frac{d^2}{dR^2} + U + \frac{N^+(N^+ + 1)}{2\mu_{\text{rot}}R^2} - E_i \right] \phi_i = 0, \quad (2)$$

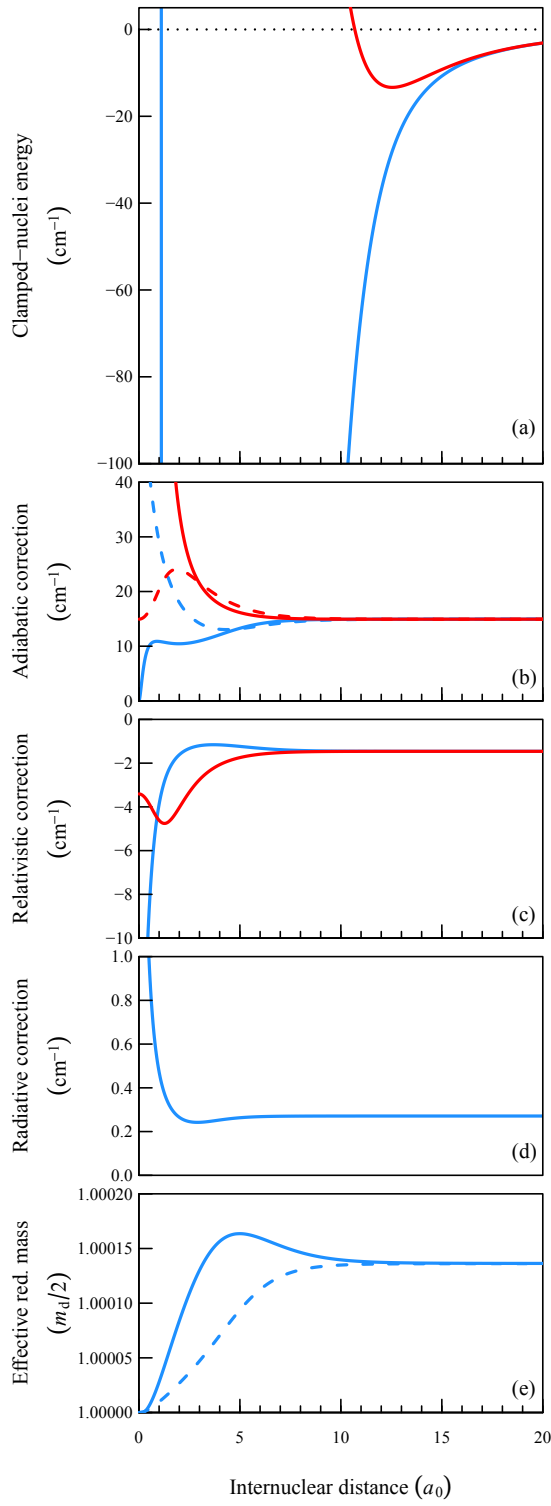


FIG. 2. (a) Clamped-nuclei (Born-Oppenheimer) potential-energy functions of the $X^+ \ ^2\Sigma_g^+$ and $A^+ \ ^2\Sigma_u^+$ states of D_2^+ calculated in this work with respect to the dissociation energy (dotted line). (b) H_1 (full lines) and H_2 (dashed lines) adiabatic corrections. (c) Relativistic corrections. (d) Radiative correction for the X^+ state. (e) Effective reduced-mass functions for the vibrational (full lines) and rotational (dashed lines) motions used to evaluate the nonadiabatic corrections of the X^+ state of D_2^+ taken from the work of Jaquet and Kutzelnigg [22] (blue). In (a)-(c), the functions drawn in blue and red color are for the X^+ and A^+ states, respectively.

where E_i and ϕ_i denote the energy and vibrational wavefunction of state i , respectively. For calculations at various levels of approximation, we used (BO = Born-Oppenheimer, AD = adiabatic, NA = nonadiabatic approximation)

$$\text{BO : } U = U^{\text{BO}}, \mu_{\text{vib}} = \mu_{\text{rot}} = \frac{m_{\text{d}}}{2}, \quad (3)$$

$$\text{AD : } U = U^{\text{BO}} + \langle H'_1 \rangle + \langle H'_2 \rangle, \mu_{\text{vib}} = \mu_{\text{rot}} = \frac{m_{\text{d}}}{2}, \quad (4)$$

$$\begin{aligned} \text{X}^+ \text{ NA : } U &= U^{\text{BO}} + \langle H'_1 \rangle + \langle H'_2 \rangle, \\ \mu_{\text{vib}}^{-1} &= \mu^{-1} (1 + A_{\mu}/m_{\text{d}}), \quad \mu_{\text{rot}}^{-1} = \mu^{-1} (1 + B_{\mu,\text{pol}}/m_{\text{d}}), \end{aligned} \quad (5)$$

$$\text{A}^+ \text{ NA : } U = U^{\text{BO}} + \langle H'_1 \rangle + \langle H'_2 \rangle, \mu_{\text{vib}} = \mu_{\text{rot}} = \frac{m_{\text{d}}(m_{\text{d}} + 1)}{2m_{\text{d}} + 1}, \quad (6)$$

with the adiabatic corrections given by

$$\begin{aligned} \langle H'_1 \rangle (R) &= \int \psi_s^*(r; R) \left[-\frac{\nabla_R^2}{2\mu} \right] \psi_s(r; R) d\tau \\ \langle H'_2 \rangle (R) &= \int \psi_s^*(r; R) \left[-\frac{\nabla_r^2}{8\mu} \right] \psi_s(r; R) d\tau. \end{aligned} \quad (7)$$

In Eqs. (2)-(7), $\psi_s(r; R)$ is the electronic BO wavefunction, μ is the reduced mass and the other symbols have their usual meaning. A_{μ} and $B_{\mu,\text{pol}}$ were taken from Ref. 22 to incorporate nonadiabatic corrections while retaining a single-potential description.

For the relativistic corrections, we evaluated the following terms of order $(R_{\infty}\alpha^2)$ [12, 24]

$$\langle H_{\text{rel}} \rangle (R) = \alpha^2 \left\langle -\frac{\mathbf{p}_e^4}{8} + \frac{4\pi}{8} [\delta(\mathbf{r}_a) + \delta(\mathbf{r}_b)] \right\rangle, \quad (8)$$

where \mathbf{r}_a and \mathbf{r}_b give the position of the electron relative to the two nuclei, \mathbf{p}_e is the momentum operator of the electron and $\delta(\mathbf{r})$ is Dirac's delta function. For the X^+ state, radiative corrections were included up to terms of order $(R_{\infty}\alpha^3)$ [12],

$$\langle H_{\text{rad}} \rangle (R) = \frac{4\alpha^3}{3} \left[\ln \frac{1}{\alpha^2} - \beta + \frac{19}{30} \right] \langle \delta(\mathbf{r}_a) + \delta(\mathbf{r}_b) \rangle, \quad (9)$$

where β is the Bethe logarithm [25, 26]. Radiative corrections were not determined for the A^+ state.

At the accuracy level of our measurements, terms of order $(R_{\infty}\alpha^2/m_{\text{d}})$ and $(R_{\infty}\alpha^3/m_{\text{d}})$ for the relativistic and radiative corrections, respectively, can be neglected. This also applies to the asymptotic values of the relativistic and radiative corrections, for which we used mass-(isotope)-independent values, in contrast to Moss [8], who scaled the expectation value of the Dirac delta function for the different isotopes, as explained in Ref. 27. The effects of this scaling are already larger than the one-transverse-photon-exchange term, which scales as $(R_{\infty}\alpha^3/m_{\text{d}})$ and is neglected here and in Refs. 8 and 25.

The Born-Oppenheimer potential energy curves of the X^+ and A^+ states and the different corrections discussed above are depicted in Fig. 2 (a)-(d), where one sees that the corrections reach their asymptotic values for the H atom at $R \approx 10 a_0$. This is also true for the R -dependent reduced masses for the X^+ state as shown in Fig. 2 (e), which justifies the use of the atomic reduced mass in the calculation of rovibrational levels of the A^+ state (see Eq. (6)).

Dissociation energies were obtained by subtracting the corresponding asymptotic energy of the deuterium atom from the calculated level energies using

$$E_{\text{D}}^{(\text{BO})} = -1/2 \quad (10)$$

$$E_{\text{D}}^{(\text{AD})} = \frac{1 - m_{\text{d}}}{2m_{\text{d}}} \quad (11)$$

$$E_{\text{D}}^{(\text{NA})} = -\frac{1}{2(1 + m_{\text{d}}^{-1})} \quad (12)$$

$$E_{\text{D}}^{(\text{NA,rel,rad})} = \left[-\frac{1}{2(1 + m_{\text{d}}^{-1})} + \frac{(-1.46092 + 0.27110) \text{ cm}^{-1}}{2\mathcal{R}_{\infty}} \right], \quad (13)$$

where \mathcal{R}_{∞} is Rydberg's constant in cm^{-1} .

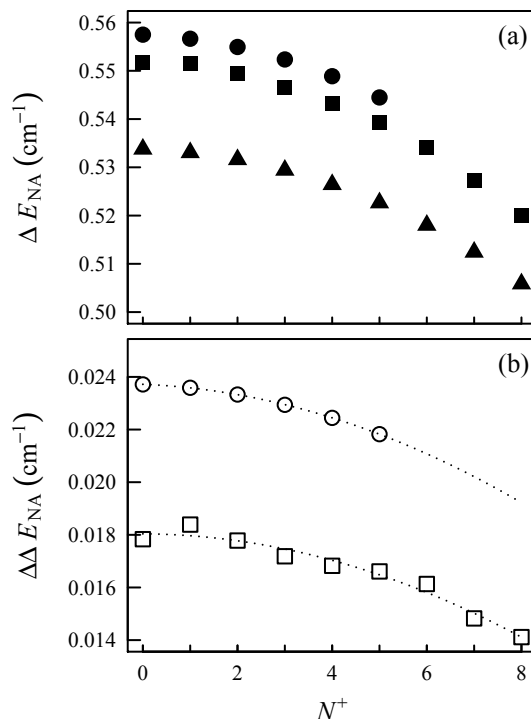


FIG. 3. (a) Nonadiabatic corrections of the dissociation energies of the rotational levels of the $X^+ \ ^2\Sigma_g^+(v^+ = 20)$ level of D_2^+ . Circles: values calculated using an artificial-channel approach by Moss [8]; squares: values derived from the perturbation-variational calculations of Wolniewicz and Orlikowski [7] (see text); triangles: values calculated in the present work using the R -dependent reduced masses of Jaquet and Kutzelnigg [22]. (b) Differences between the nonadiabatic corrections calculated in the present work and those reported by Moss [8] (open circles) and by Wolniewicz and Orlikowski [7] (open squares). The dotted lines represent a fit to the data (see text for details).

The theoretical results for the total dissociation energies and the contributions from the different correction terms are listed in Tables I and II, where they are compared with the experimental results and the total dissociation energies calculated by Moss [8] and Wolniewicz and Orlikowski [7]. The comparison of the theoretical results indicate that the differences originate almost exclusively from the nonadiabatic corrections, which were calculated exactly in Refs. 7 and 8 but only approximately in the present work using the effective R -dependent reduced masses derived by Kutzelnigg and Jaquet [22]. The approach of Kutzelnigg and Jaquet, which includes only the effects of the first excited states of $^2\Sigma_g^+$ and $^2\Pi_g$ symmetry, is computationally efficient and allows one to retain a single-potential description of the electronic states, which offers advantages in the calculations and interpretation of shape resonances [17, 18]. All corrections in Tables I and II tend towards zero as the level energies approach the dissociation limit, as expected.

Fig. 3a compares our values for the nonadiabatic corrections ΔE_{NA} (triangles) for the dissociation energies of the X^+ ($v^+ = 20, N^+ = 0 - 10$) levels of D_2^+ with the nonadiabatic corrections calculated by Moss [8] for levels with $N^+ \leq 5$ (circles) and the nonadiabatic corrections we derived from the total energies of Wolniewicz and Orlikowski [7] by subtracting all other contributions (squares). The nonadiabatic corrections to the dissociation energies are about 0.5 cm^{-1} and decrease with increasing N^+ values. The differences $\Delta\Delta E_{\text{NA}}$ between our approximate values and the values reported by Moss [8] and Wolniewicz and Orlikowski [7] do not exceed 0.025 cm^{-1} (i.e., they are less than 5%) and are drawn on an enlarged scale in Fig. 3b as a function of N^+ . The comparison shows that the errors $\Delta\Delta E_{\text{NA}}$ caused by our approximate treatment of the nonadiabatic correction are linear in $N^+(N^+ + 1)$ and do not deviate by more than 0.017 cm^{-1} at $N^+ = 10$ from the values one can extrapolate using the results of Moss [8]. The large discrepancy for $N^+ = 0$ and the weak N^+ -dependence of $\Delta\Delta E_{\text{NA}}$ suggests that it is mainly the Σ nonadiabatic corrections that are underestimated using the effective reduced masses.

The treatment of nonadiabatic corrections through effective reduced masses is not a necessity in H_2^+ , HD^+ and D_2^+ because they can be calculated with almost arbitrary precision by variational or other methods [7, 8, 10–12]. In molecules with a larger number of electrons, however, exact nonadiabatic calculations are more demanding and the use of R -dependent effective reduced masses, derived from LCAO wavefunctions, becomes more attractive. In a recent computation of the energy levels of He_2^+ , for instance, Tung *et al.* [28] have relied on R -independent effective

reduced masses to treat the nonadiabatic corrections. The resulting rotational level energies of the $X^+ \ ^2\Sigma_u^+(v^+ = 0)$ ground state of He_2^+ were found to deviate from experimental results [29], the deviations increasing quadratically with N^+ . On the basis of the present results on D_2^+ we suspect that the deviation mainly comes from an incomplete treatment of the nonadiabatic corrections in Ref. 28. H_2^+ , HD^+ and D_2^+ are ideal systems to quantify the effects of the approximations by comparison with exact calculations.

Most corrections to the dissociation energies listed in Tables I and II are larger than the 0.02 cm^{-1} uncertainties of the experimental values. The corrections given in the tables represent energy differences between the $\text{D}^+ + \text{D}(1s)$ dissociation limit and the bound levels. Only the radiative corrections are consistently less than the experimental uncertainties and can thus not be checked by comparison with the measured ionic level intervals. The corrections of the absolute term value with respect to the X state of the D_2^+ levels are much larger. Depending on the level considered, the adiabatic, nonadiabatic, relativistic and radiative corrections can be as large as 30 cm^{-1} , 0.65 cm^{-1} , 1.6 cm^{-1} , and 0.35 cm^{-1} (see Fig. 2). Accordingly all corrections have to be taken into account to compare calculated [4] and measured absolute term values.

IV. EXPERIMENTAL RESULTS

The PFI-ZEKE photoelectron spectra of D_2 recorded via the $\bar{\text{H}}(v = 12, N = 2)$ and $\bar{\text{H}}(v = 12, N = 3)$ intermediate levels are displayed in Fig. 4a and b, respectively. The spectra consist of transitions to bound levels of D_2^+ located up to 1400 cm^{-1} below the $\text{D}(1s) + \text{D}^+$ dissociation threshold. The transitions can be grouped in rotational progressions associated with the $v^+ = 20 - 26$ vibrational levels of the $X^+ \ ^2\Sigma_g^+$ state and the $v^+ = 0, 1$ vibrational levels of the $A^+ \ ^2\Sigma_u^+$ state. The spacings between the successive vibrational progressions of the X^+ state and between adjacent rotational levels of a given progression rapidly decrease with increasing v^+ value, so that the density of states close to the dissociative ionization threshold, where transitions to the X^+ and A^+ levels overlap, is high.

The intensity distributions within the different progressions are irregular and rapidly change with the value of v^+ . This behavior reflects the facts that (i) the vibrational wavefunctions of the ion and thus the vibrational overlap integrals with the $\bar{\text{H}}(12, N)$ wavefunctions depend on N^+ through the centrifugal term in the nuclear Schrödinger equation, and (ii) the electronic transition moment from the $\bar{\text{H}}$ state to the X^+ and A^+ ionization channels depend strongly on the internuclear distance R , reflecting the R dependence of the electronic character of the $\bar{\text{H}}$ state. Whereas this state has ion-pair character at long range, with both electrons located on the same D atom, it gains repulsive $(2p\sigma_u)(3p\sigma_u)$ character as R is reduced towards the inner well (H state).

The ion-pair character of the $\bar{\text{H}}$ state also leads to large changes ($\Delta N = |N^+ - N|$ up to 6) of the rotational quantum number upon ionization, which is much larger than for the ionization of valence or low-lying Rydberg states of molecular hydrogen [30, 31]. The orbital out of which the electron is ejected has the character of an s orbital centered on H^- . A single center expansion of this orbital around the geometric center of the molecule is expected not to converge fast with increasing value of the orbital angular-momentum quantum number l and thus to give rise to large $|\Delta N|$ values according to the propensity rule for photoionization

$$\Delta N \leq |l| \quad (14)$$

obtained using the orbital-ionisation approximation [32, 33]. The rotational progressions observed experimentally all obey the selection rule $\Delta N = \text{even or odd}$ for transitions to the $X^+ \ ^2\Sigma_g^+$ or $A^+ \ ^2\Sigma_u^+$ state, respectively, which is imposed by the conservation of nuclear-spin symmetry. The spectra depicted in Fig. 4 do not reveal any transition associated with a conversion of ortho and para D_2 .

Tables I and II list the positions of the observed levels of ortho D_2^+ relative to that of the $X^+(23,4)$ level, and of para D_2^+ relative to that of the $X^+(20,1)$ level, respectively. These positions were determined from the statistical analysis of multiple recordings of PFI-ZEKE photoelectron spectra measured from different rotational levels of the $\bar{\text{H}}(v = 12)$ intermediate state and by collecting the electrons produced by different pulses of the field-ionization sequence in separate time-of-flight windows (see Section II).

More than 1600 lines were included in the analysis, corresponding to more than 160 distinct photoionizing transitions connecting the $\bar{\text{H}}(v = 12, N = 0 - 6)$ intermediate levels to 70 rovibronic levels of D_2^+ . The reference levels chosen for ortho D_2^+ ($X^+(23,4)$) and para D_2^+ ($X^+(20,1)$) are those that are best defined by the network of observed transitions, as determined in a weighted linear least-squares fit of the level positions to the observed transition wave numbers. The least-squares fit also yielded the relative positions of the rotational levels of the $\bar{\text{H}}(v = 12)$ state, as summarized in Table III, where they are compared with the earlier results of Reinhold *et al.* [21]. The uncertainties of typically 0.02 cm^{-1} are about five times less than the full width at half maximum of the narrowest lines observed experimentally.

The positions of the D_2^+ levels could also be determined with respect to the rotational levels of the $\bar{\text{H}}(v = 12)$ state, and, by using the $\bar{\text{H}}(v = 12, N)$ term values reported by Reinhold *et al.* [21], also to the X (0,0) ground state of D_2 .

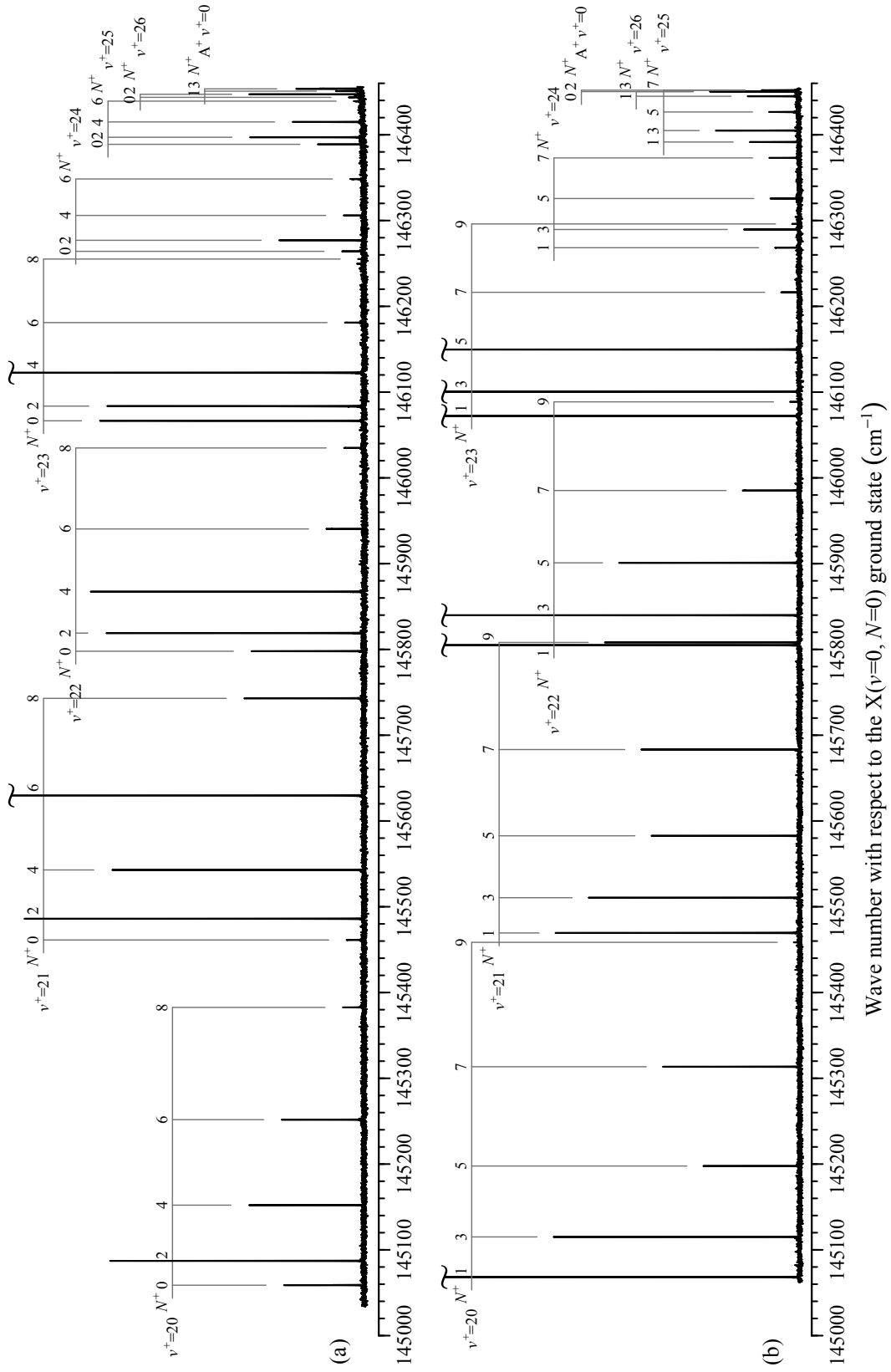


FIG. 4. PFI-ZEKE photoelectron spectra of D_2 recorded near the dissociative-ionization threshold from (a) the $\bar{H}(v=12, N=2)$ level and (b) the $\bar{H}(v=12, N=3)$ level. The vertical scale is linear and in arbitrary units.

TABLE I. Measured level positions and dissociation energies of ortho D_2^+ with respect to the $X^+(23,4)$ level and adiabatic, nonadiabatic, relativistic and radiative corrections to the dissociation energies. All values are in cm^{-1} and the experimental uncertainties represent one standard deviation.

	v^+	N^+	Obs.	Lit.	This work	ΔE_{AD}	ΔE_{NA}	ΔE_{rel}	ΔE_{rad}
X^+	20	0	-1063.782(18)	-1063.7728 [8]	-1063.7695	2.0352	0.5338	-0.0680	-0.0038
X^+	20	2	-1035.515(16)	-1035.5286 [8]	-1035.5257	2.0267	0.5316	-0.0683	-0.0036
X^+	20	4	-970.516(16)	-970.5281 [8]	-970.5261	2.0062	0.5264	-0.0689	-0.0033
X^+	20	6	-870.901(17)	-870.909 [7]	-870.9103	1.9726	0.5180	-0.0698	-0.0027
X^+	20	8	-739.981(21)	-739.970 [7]	-739.9741	1.9241	0.5059	-0.0706	-0.0020
X^+	21	0	-661.364(21)	-661.3706 [8]	-661.3669	1.7840	0.4803	-0.0615	-0.0025
X^+	21	2	-636.595(16)	-636.6011 [8]	-636.5977	1.7732	0.4774	-0.0617	-0.0024
X^+	21	4	-579.720(16)	-579.7267 [8]	-579.7243	1.7474	0.4707	-0.0619	-0.0021
X^+	21	6	-492.940(15)	-492.938 [7]	-492.9386	1.7052	0.4596	-0.0620	-0.0016
X^+	21	8	-379.638(17)	-379.638 [7]	-379.6406	1.6444	0.4437	-0.0619	-0.0010
X^+	22	0	-324.643(16)	-324.6655 [8]	-324.6625	1.5026	0.4140	-0.0533	-0.0015
X^+	22	2	-303.581(16)	-303.5735 [8]	-303.5708	1.4892	0.4104	-0.0532	-0.0014
X^+	22	4	-255.306(16)	-255.3146 [8]	-255.3128	1.4574	0.4017	-0.0530	-0.0011
X^+	22	6	-182.147(19)	-182.174 [7]	-182.1749	1.4053	0.3875	-0.0524	-0.0007
X^+	22	8	-87.730(21)	-87.739 [7]	-87.7420	1.3301	0.3671	-0.0512	-0.0003
X^+	23	0	-56.171(17)	-56.1762 [8]	-56.1750	1.1896	0.3341	-0.0432	-0.0007
X^+	23	2	-39.033(15)	-39.0185 [8]	-39.0177	1.1732	0.3295	-0.0429	-0.0006
X^+	23	4	0 ^a	0 ^b [8]	0 ^c	1.1343	0.3185	-0.0421	-0.0004
X^+	23	6	58.379(21)	58.428 [7]	58.4267	1.0703	0.3005	-0.0408	-0.0001
X^+	23	8	132.36(9)	132.350 [7]	132.3467	0.9773	0.2743	-0.0384	0.0002
X^+	23	10	216.19(5)	—	216.1853	0.8473	0.2377	-0.0346	0.0005
X^+	24	0	141.469(19)	141.4414 [8]	141.4394	0.8446	0.2400	-0.0312	-0.0002
X^+	24	2	154.346(17)	154.3372 [8]	154.3349	0.8248	0.2342	-0.0307	-0.0001
X^+	24	4	183.295(18)	183.3059 [8]	183.3027	0.7772	0.2204	-0.0294	-0.0000
X^+	24	6	225.616(17)	225.596 [7]	225.5911	0.6982	0.1976	-0.0271	0.0002
X^+	24	8	276.65(3)	276.628 [7]	276.6209	0.5803	0.1634	-0.0233	0.0004
X^+	24	10	329.20(3)	—	329.1478	0.4019	0.1117	-0.0169	0.0005
X^+	25	0	266.188(17)	266.1669 [8]	266.1608	0.4753	0.1339	-0.0179	0.0001
X^+	25	2	274.422(16)	274.4073 [8]	274.4007	0.4515	0.1268	-0.0172	0.0001
X^+	25	4	292.327(16)	292.3194 [8]	292.3119	0.3940	0.1098	-0.0152	0.0002
X^+	25	6	316.544(17)	316.513 [7]	316.5164	0.2957	0.0807	-0.0118	0.0002
X^+	26	0	321.064(16)	321.0491 [8]	321.0386	0.1426	0.0349	-0.0055	0.0001
X^+	26	2	324.596(15)	324.5783 [8]	324.5675	0.1209	0.0284	-0.0048	0.0001
X^+	26	4	331.33(3)	331.3033 [8]	331.2918	0.0696	0.0130	-0.0028	0.0001
A^+	0	1	328.264(16)	328.2367 [8]	328.2195	0.0032	-0.0077	-0.0004	—
A^+	0	3	330.93(3)	330.9055 [8]	330.8888	0.0035	-0.0074	-0.0004	—

^aCorresponds to an absolute term value of $146123.81(11) \text{ cm}^{-1}$ [this work].

^bCorresponds to a dissociation energy of 333.1893 cm^{-1} [8] and 333.185 cm^{-1} [7].

^cCorresponds to a dissociation energy of 333.1688 cm^{-1} [this work].

This was achieved in a statistical analysis of the field-induced shifts of the ionization thresholds associated with the different pulses of the field-ionization sequence using numerical simulations of the field-ionization process, as described in Ref. 20. In this way, we could determine the absolute term values (i.e., their wave number above the $X(0,0)$ ground state of D_2) of the two reference levels in Tables I and II to be $146123.81(11) \text{ cm}^{-1}$ and $145069.47(11) \text{ cm}^{-1}$ for the $X^+(23,4)$ and $X^+(20,1)$ levels, respectively. The uncertainty of 0.11 cm^{-1} in these values is dominated by the uncertainty in the field-induced shifts (0.1 cm^{-1}), and to a lesser extent by the uncertainties (0.04 cm^{-1}) of the $\bar{H}(v = 12, N)$ term values reported by Reinhold *et al.* [21].

At the resolution of 0.1 cm^{-1} of the photoelectron spectra, we could not observe the hyperfine structure of the D_2^+

TABLE II. Measured level positions and dissociation energies of para D_2^+ with respect to the $X^+(20,1)$ level and adiabatic, nonadiabatic, relativistic and radiative corrections to the dissociation energies. All values are in cm^{-1} and the experimental uncertainties represent one standard deviation.

	v^+	N^+	Obs.	Lit.	This work	ΔE_{AD}	ΔE_{NA}	ΔE_{rel}	ΔE_{rad}
X^+	20	1	0 ^a	0 ^b [8]	0 ^c	2.0324	0.5331	-0.0681	-0.0037
X^+	20	3	46.804(16)	46.8152 [8]	46.8145	2.0180	0.5294	-0.0686	-0.0035
X^+	20	5	129.462(16)	129.4653 [8]	129.4635	1.9911	0.5227	-0.0693	-0.0030
X^+	20	7	245.220(16)	245.226 [7]	245.2211	1.9504	0.5124	-0.0702	-0.0024
X^+	20	9	390.23(9)	—	390.2388	1.8934	0.4982	-0.0709	-0.0016
X^+	21	1	401.240(16)	401.2445 [8]	401.2449	1.7804	0.4793	-0.0616	-0.0025
X^+	21	3	442.259(16)	442.2635 [8]	442.2632	1.7622	0.4746	-0.0618	-0.0022
X^+	21	5	514.436(16)	514.4445 [8]	514.4432	1.7284	0.4657	-0.0620	-0.0018
X^+	21	7	614.990(16)	614.988 [7]	614.9840	1.6773	0.4523	-0.0620	-0.0013
X^+	21	9	739.895(16)	—	739.8947	1.6060	0.4337	-0.0616	-0.0007
X^+	22	1	736.729(15)	736.7247 [8]	736.7245	1.4982	0.4128	-0.0532	-0.0015
X^+	22	3	771.590(15)	771.6048 [8]	771.6040	1.4757	0.4067	-0.0531	-0.0013
X^+	22	5	832.672(16)	832.6707 [8]	832.6687	1.4340	0.3953	-0.0527	-0.0009
X^+	22	7	917.021(17)	916.987 [7]	916.9839	1.3708	0.3781	-0.0519	-0.0005
X^+	22	9	1020.344(24)	—	1020.3065	1.2825	0.3541	-0.0503	-0.0000
X^+	23	1	1003.923(16)	1003.9042 [8]	1003.9021	1.1842	0.3326	-0.0431	-0.0007
X^+	23	3	1032.218(16)	1032.2103 [8]	1032.2075	1.1567	0.3248	-0.0426	-0.0005
X^+	23	5	1081.337(16)	1081.3293 [8]	1081.3254	1.1056	0.3104	-0.0415	-0.0003
X^+	23	7	1148.081(21)	1148.089 [7]	1148.0847	1.0278	0.2885	-0.0397	0.0000
X^+	23	9	1227.82(4)	—	1227.7799	0.9176	0.2575	-0.0367	0.0004
X^+	24	1	1200.113(19)	1200.1040 [8]	1200.0988	0.8381	0.2381	-0.0311	-0.0002
X^+	24	3	1221.278(18)	1221.2777 [8]	1221.2718	0.8046	0.2284	-0.0302	-0.0001
X^+	24	5	1257.370(20)	1257.3566 [8]	1257.3495	0.7420	0.2102	-0.0284	0.0001
X^+	24	7	1304.741(20)	1304.721 [7]	1304.7137	0.6449	0.1821	-0.0254	0.0003
X^+	24	9	1357.65(3)	—	1357.6448	0.5015	0.1406	-0.0205	0.0004
X^+	25	1	1323.291(17)	1323.2828 [8]	1323.2733	0.4674	0.1315	-0.0177	0.0001
X^+	25	3	1336.651(16)	1336.6446 [8]	1336.6345	0.4273	0.1196	-0.0164	0.0001
X^+	25	5	1358.291(16)	1358.2754 [8]	1358.2641	0.3508	0.0970	-0.0138	0.0002
X^+	25	7	1383.62(15)	1383.469 [7]	1383.4603	0.2244	0.0596	-0.0092	0.0002
X^+	26	1	1376.598(16)	1376.5987 [8]	1376.5850	0.1354	0.0327	-0.0053	0.0001
X^+	26	3	1382.06(5) ^d	1382.0618 [8]	1382.0475	0.0992	0.0218	-0.0040	0.0001
A^+	0	0	1382.06(5) ^d	1382.0081 [8]	1381.9927	0.0031	-0.0077	-0.0004	—
A^+	0	2	1383.654(16)	1383.6650 [8]	1383.6496	0.0034	-0.0075	-0.0004	—
A^+	1	0	1387.179(20)	1387.2130 [8]	1387.1976	0.0007	-0.0080	-0.0001	—

^aCorresponds to an absolute term value of $145069.47(11) \text{ cm}^{-1}$ [this work].

^bCorresponds to a dissociation energy of $1387.5215 \text{ cm}^{-1}$ [8] and 1387.516 cm^{-1} [7].

^cCorresponds to a dissociation energy of $1387.4979 \text{ cm}^{-1}$ [this work].

^dBlended line.

levels, which is expected to be about 0.006 cm^{-1} [16]. The values given in Tables I and II thus correspond to the pure rovibronic level energies.

The comparison of the relative positions of the D_2^+ levels with the values calculated *ab initio* by Moss [8] and Wolniewicz and Orlikowski [7] are overall in agreement within the experimental uncertainties. Less than 30% of the experimental wave numbers lie further away from the theoretical results than their experimental standard deviations. The square root of the sum of squared deviations of the experimental from these calculated results (0.189 cm^{-1}) is smaller than the square root of the sum of squared deviations from the levels we calculated using the approximate treatment of the nonadiabatic corrections through R -dependent reduced masses described above (0.208 cm^{-1}). The residuals indicate that the approximation slightly underestimates the nonadiabatic corrections, as expected from the

TABLE III. Rotational term values of the $\bar{\text{H}} \ ^1\Sigma_g^+(v = 12)$ state. All values are in cm^{-1} and the experimental uncertainties represent one standard deviation.

N	obs.	Lit. [21]
0	0	0
2	2.909(19)	2.92(6)
4	9.713(20)	9.69(6)
6	20.361(21)	–
1	0	0
3	4.854(21)	4.83(6)
5	13.585(14)	13.62(6)

results presented in Section III (see Fig. 3).

V. CONCLUSIONS

The data presented in this article considerably extend the experimental knowledge of the rovibrational levels of D_2^+ . Good agreement was found between the measured dissociation energies of these levels with the results of *ab initio* quantum-chemical calculations that take into account adiabatic, nonadiabatic, relativistic and radiative corrections. All corrections except for the radiative ones are required to reach agreement at the 0.02 cm^{-1} precision level for the relative ionic intervals measured in this experiment (see Tables I and II). Even the radiative corrections have to be included to account for the absolute term values of the D_2^+ levels with respect to the neutral ground state. For instance, the radiative correction of the $\text{X}^+(20, 1)$ level determined as the sum and difference of the radiative corrections of the dissociation energy of D_2 (-0.1983 cm^{-1} [4]), the ionization energy of D (-0.2709 cm^{-1} [34]) and the dissociation energy of the $\text{X}^+(20, 1)$ level, is -0.4654 cm^{-1} , which is four times as large as the uncertainty of our absolute term values. This study thus represents the first example of a determination of effects resulting from the field quantization by photoelectron spectroscopy. Approximating the nonadiabatic corrections using effective R -dependent reduced masses was found to be efficient and to introduce errors of less than 5% compared to corrections calculated exactly.

Photoionization through an intermediate state with ion-pair character was found to be an efficient way of observing a wide range of rotational states of the ion. The spectra of the bound levels of D_2^+ do not reveal any sign of g/u -mixing by the hyperfine interaction within the sensitivity of our measurement. The present results provide the basis for the treatment of the resonances of D_2^+ above the $\text{D}(1s)+\text{D}^+$ dissociation limit, which we are currently studying [35].

A. Acknowledgments

We thank Prof. V. Korobov (Dubna) for stimulating discussions and for providing extended tables with the values of the Bethe logarithm and the mass variable correction. This work was supported financially by the Swiss National Science Foundation (Project No. 200020-172620) and the European Research Council (ERC) under the European Union’s Horizon 2020 research and innovation programme (Advanced Grant 743121).

-
- [1] P. Quadrelli, K. Dressler, and L. Wolniewicz, “Nonadiabatic coupling between the $\text{EF}+\text{GK}+\text{H} \ ^1\Sigma_g^+$, $\text{I} \ ^1\Pi_g$, and $\text{J} \ ^1\Delta_g$ states of the hydrogen molecule. calculation of rovibronic structures in H_2 , HD , and D_2 ,” *J. Chem. Phys.* **92**, 7461 (1990).
 - [2] S. C. Ross and C. Jungen, “Multichannel quantum-defect theory of $n = 2$ and 3 gerade states in H_2 : Rovibronic energy levels,” *Phys. Rev. A* **50**, 4618 (1994).
 - [3] M. Sommovilla, F. Merkt, J. Z. Mezei, and C. Jungen, “Absorption, autoionization, and predissociation in molecular hydrogen: High-resolution spectroscopy and multichannel quantum defect theory,” *J. Chem. Phys.* **144**, 084303 (2016).
 - [4] K. Piszczatowski, G. Lach, M. Przybytek, J. Komasa, K. Pachucki, and B. Jeziorski, “Theoretical Determination of the Dissociation Energy of Molecular Hydrogen,” *J. Chem. Theory Comput.* **5**, 3039 (2009).
 - [5] K. Pachucki and J. Komasa, “Leading order nonadiabatic corrections to rovibrational levels of H_2 , D_2 , and T_2 ,” *J. Chem. Phys.* **143**, 034111 (2015).

- [6] K. Pachucki and J. Komasa, “Schrödinger equation solved for the hydrogen molecule with unprecedented accuracy,” *J. Chem. Phys.* **144**, 164306 (2016).
- [7] L. Wolniewicz and T. Orlikowski, “The $1s\sigma_g$ and $2p\sigma_u$ states of the H_2^+ , D_2^+ and HD^+ ions,” *Mol. Phys.* **74**, 103 (1991).
- [8] R. E. Moss, “The $2p\sigma_u - 1s\sigma_g$ electronic spectrum of D_2^+ ,” *J. Chem. Soc., Faraday Trans.* **89**, 3851 (1993).
- [9] C. A. Leach and R. E. Moss, “Spectroscopy and Quantum Mechanics of the Hydrogen Molecular Cation: A Test of Molecular Quantum Mechanics,” *Annu. Rev. Phys. Chem.* **46**, 55 (1995).
- [10] J. M. Taylor, Z.-C. Yan, A. Dalgarno, and J. F. Babb, “Variational calculations on the hydrogen molecular ion,” *Mol. Phys.* **97**, 25 (1999).
- [11] L. Hilico, N. Billy, B. Grémaud, and D. Delande, “Ab initio calculation of the $J = 0$ and $J = 1$ states of the H_2^+ , D_2^+ and HD^+ molecular ions,” *Eur. Phys. J. D* **12**, 449 (2000).
- [12] V. I. Korobov, “Leading-order relativistic and radiative corrections to the rovibrational spectrum of H_2^+ and HD^+ molecular ions,” *Phys. Rev. A* **74**, 052506 (2006).
- [13] A. Carrington, I. R. McNab, C. A. Montgomerie, and R. A. Kennedy, “Electronic spectrum $2p\sigma_u - 1s\sigma_g$ of the D_2^+ ion,” *Mol. Phys.* **67**, 711 (1989).
- [14] A. Carrington, I. R. McNab, C. A. Montgomerie, and J. M. Brown, “Microwave spectra of the HD^+ and D_2^+ ions at their dissociation limits,” *Mol. Phys.* **66**, 1279 (1989).
- [15] A. Carrington, C. A. Leach, A. J. Marr, R. E. Moss, C. H. Pyne, and T. C. Steimle, “Microwave spectra of the D_2^+ and HD^+ ions near their dissociation limits,” *J. Chem. Phys.* **98**, 5290 (1993).
- [16] H. A. Cruse, C. Jungen, and F. Merkt, “Hyperfine structure of the ground state of para- D_2^+ by high-resolution Rydberg-state spectroscopy and multichannel quantum defect theory,” *Phys. Rev. A* **77**, 042502 (2008).
- [17] M. Beyer and F. Merkt, “Observation and Calculation of the Quasibound Rovibrational Levels of the Electronic Ground State of H_2^+ ,” *Phys. Rev. Lett.* **116**, 093001 (2016).
- [18] M. Beyer and F. Merkt, “Structure and dynamics of H_2^+ near the dissociation threshold: A combined experimental and computational investigation,” *J. Mol. Spectrosc.* **330**, 147 (2016); The reduced mass in Eq. (15) of this article should read:

$$\mu_{\text{vib}} = \mu_{\text{rot}} = \frac{m_p(m_p+1)}{2m_p+1} .$$
- [19] S. A. Astashkevich and B. P. Lavrov, “Lifetimes of vibro-rotational levels in excited electronic states of diatomic hydrogen isotopologues,” *J. Phys. Chem. Ref. Data* **44**, 023105 (2015).
- [20] U. Hollenstein, R. Seiler, H. Schmutz, M. Andrist, and F. Merkt, “Selective field ionization of high Rydberg states: Application to zero-kinetic-energy photoelectron spectroscopy,” *J. Chem. Phys.* **115**, 5461 (2001).
- [21] E. Reinhold, W. Hogervorst, W. Ubachs, and L. Wolniewicz, “Experimental and theoretical investigation of the $H\bar{H} \ ^1\Sigma_g^+$ state in H_2 , D_2 , and HD , and the $B''\bar{B} \ ^1\Sigma_u^+$ state in HD ,” *Phys. Rev. A* **60**, 1258 (1999).
- [22] R. Jaquet and W. Kutzelnigg, “Non-adiabatic theory in terms of a single potential energy surface. The vibration-rotation levels of H_2^+ and D_2^+ ,” *Chem. Phys.* **346**, 69 (2008).
- [23] P. J. Mohr, B. N. Taylor, and D. B. Newell, *The 2014 CODATA Recommended Values of the Fundamental Physical Constants (Web Version 7.0). This database was developed by J. Baker, M. Douma, and S. Kotochigova. National Institute of Standards and Technology, Gaithersburg, MD 20899, <http://physics.nist.gov/constants>.*
- [24] T. Tsogbayar and V. I. Korobov, “Relativistic correction to the $1s\sigma$ and $2p\sigma$ electronic states of the H_2^+ molecular ion and the moleculelike states of the antiprotonic helium $He^+\bar{p}$,” *J. Chem. Phys.* **125**, 024308 (2006).
- [25] R. Bukowski, B. Jeziorski, R. Moszyński, and W. Kolos, “Bethe logarithm and Lamb shift for the hydrogen molecular ion,” *Int. J. Quant. Chem.* **42**, 287 (1992).
- [26] V. I. Korobov, “Bethe logarithm for the hydrogen molecular ion H_2^+ ,” *Phys. Rev. A* **73**, 024502 (2006).
- [27] H. A. Bethe and E. E. Salpeter, “Quantum mechanics of one- and two-electron atoms,” (Springer Verlag, 1957) p. 101.
- [28] W.-C. Tung, M. Pavanello, and L. Adamowicz, “Very accurate potential energy curve of the He_2^+ ion,” *J. Chem. Phys.* **136**, 104309 (2012).
- [29] L. Semeria, P. Jansen, and F. Merkt, “Precision measurement of the rotational energy-level structure of the three-electron molecule He_2^+ ,” *J. Chem. Phys.* **145**, 204301 (2016).
- [30] L. Åsbrink, “The photoelectron spectrum of H_2 ,” *Chem. Phys. Lett.* **7**, 549 (1970).
- [31] F. Merkt and T. P. Softley, “Final-state interactions in the zero-kinetic-energy photoelectron spectrum of H_2 ,” *J. Chem. Phys.* **96**, 4149 (1992).
- [32] A. D. Buckingham, B. J. Orr, and J. M. Sichel, “Angular Distribution and Intensity in Molecular Photoelectron Spectroscopy I. General Theory for Diatomic Molecules,” *Phil. Trans. Roy. Soc. Lond. A* **268**, 147 (1970).
- [33] J. Xie and R. N. Zare, “Selection rules for the photoionization of diatomic molecules,” *J. Chem. Phys.* **93**, 3033 (1990).
- [34] D. Sprecher, C. Jungen, W. Ubachs, and F. Merkt, “Towards measuring the ionisation and dissociation energies of molecular hydrogen with sub-MHz accuracy,” *Faraday Discuss.* **150**, 51 (2011).
- [35] M. Beyer and F. Merkt, In preparation (2017).